Static Hysteresis Modelling for Grain-Oriented Electrical Steels based on the Phenomenological Concepts of Energy Loss Mechanism

Hamed Hamzehbahmani
Department of Engineering, Durham University, Durham, DH1 3LE, UK
E-mail: Hamed.h.bahmani@durham.ac.uk

Abstract- This paper proposes an advanced approach to construct static hysteresis loop of Grain-Oriented (GO) electrical steels for dynamic modelling and energy loss analysis. The proposed approach is in line with the magnetic hysteresis and phenomenological concepts of rate-dependent and rate-independent energy loss components of ferromagnetic materials under time varying magnetic fields. The proposed method can predominantly describe energy loss mechanism and magnetization processes of the material. Accuracy of this technique was validated on Epstein size laminations of 3 % GO silicon steels. The results explicitly confirmed the effectiveness of the proposed method in dynamic hysteresis modelling of GO electrical steels at magnetizing frequencies up to 1 kHz and peak flux densities up to 1.7 T.

I.INTRODUCTION

Electrical steels are the most important soft magnetic materials in industry. They are widely used as the core materials of the rotating machines, power transformers and other electromagnetic devices installed in the electric networks and power systems. Relative permeability and total energy loss in J/m3 per cycle or specific power loss in W/kg, are two determinant parameters to characterize electrical steels for the range of magnetizations. These parameters can be effectively obtained by monitoring magnetization processes and dynamic hysteresis loop (DHL) of the material. Furthermore, coercive field H_c and residual magnetic field B_r, as two distinctive quantities of the magnetic materials, can be evaluated by monitoring DHLs [1-2]. Measuring and characterizing techniques of electrical steels are standardized in the international standard IEC 60404-2, 2008 [3], and British standard BS EN 10280:2001 + A1, 2007 [4] based on the Epstein frame and Single Strip Tester (SST), respectively. These measuring systems are widely used in industrial and academic research projects to characterize electrical steel laminations and magnetic cores. Details of the magnetization processes and magnetic hysteresis loops of the magnetic materials can be monitored with these measuring systems for a wide range magnetizations, i.e. flux densities and magnetizing frequencies.

Apart from the standard measuring systems, analytical and numerical approaches have been substantially proposed to formulate hysteresis behavior of the magnetic materials, including magnetization processes, hysteresis loops, energy loss and its components. Historical development of the mathematical models of magnetic hysteresis is appreciably reviewed in the literatures [5-7]. Amongst the proposed hysteresis models, mathematical and analytical methods based on the conventional magnetic hysteresis proposed by Preisach [8], Jiles and Atherton [9], and statistical loss separation theory proposed by Bertotti [10] are well distinguished by engineers and physicists to identify details of the magnetization processes and energy loss mechanism of the magnetic materials.

The Preisach model was proposed in 1930 to describe magnetic hysteresis of magnetic materials in terms of magnetic field H and magnetization M [8]. In this method, the material is subdivided into a number of independent small particles and each particle is modelled by a square hysteresis loop. Preisach model of hysteresis has been followed by many researchers for dynamic modelling of ferromagnetic materials, and it is the preferred technique in finite element modelling [11-13]. In 1983 Jiles and Atherton [9], developed a phenomenological hysteresis model for ferromagnetic materials based on the physical properties of the materials, e.g. magnetic dipoles, domain rotations and domain-wall motions. Jiles-Atherton model is one of the most cited and most popular methods in hysteresis modelling, due to its reduced number of parameters and its physical interpretation [14-15]. In 1988 Bertotti [10] introduced a statistical approach for power loss analysis of soft metallic ferromagnetic materials, by separating the total power loss into hysteresis loss P_{hys}, classical eddy current loss P_{eddy}, and excess loss P_{exc}. Bertotti theory provided an insight into power loss mechanism of soft magnetic materials. During the last decays, statistical loss separation theory of Bertotti has been broadly developed and implemented as a theoretical background in dynamic modelling of soft magnetic materials, amongst which work performed by Zirka et al. can be highlighted [16-18]. Zirka et al. showed that power loss separation theory can be mathematically interpreted to magnetic field separation. This theory implies that the applied magnetic field to the material can be separated

into hysteresis field H_{hys}, classical eddy current field H_{eddy}, and excess field H_{exc}. This approach is known as Thin Sheet Model (TSM) for energy loss analysis of ferromagnetic materials. TSM has been extensively used in dynamic modelling of GO electrical steels [17-18] and has found many applications in real magnetic cores, e.g. transformer modelling [19-20].

Magnetic hysteresis is a physical phenomenon to describe materials behavior and all details of the magnetization processes during each cycle of the magnetization [1-2]. Most of the phenomenological aspects of magnetic hysteresis are rate-dependent, and they can be interpreted by monitoring the DHL. Therefore, a comprehensive analysis on the dynamic behavior of the magnetic materials over a range of flux density, at a particular frequency, can provide useful information about the magnetization processes, energy loss and its components. This leads to a new insight to analyze the magnetization processes of GO electrical steels. This paper aims to perform dynamic modelling of GO steels based on the TSM, with an advanced approach to construct the static hysteresis loop (SHL). The proposed approach to construct the SHL is based on the phenomenological concepts of rate-dependent and rate-independent energy loss components of ferromagnetic materials under time-varying magnetic field. Accuracy of the proposed approach was validated for Epstein size strips of GO 3 % SiFe material at magnetizing frequencies of 50 Hz to 1 kHz and peak flux densities of 1.1 T to 1.7 T.

II. THEORY OF ENERGY LOSS MODELLING

Hysteresis phenomenon can be viewed as a phase lag between the instantaneous input and output signals in time domain. It plays a prominent role in different sciences and has been known to scientists for a long time. Hysteresis phenomenon has important implications in electromagnetism to interpret magnetizing processes, and to classify and characterize magnetic materials and electromagnetic devices. Hysteresis phenomenon is complicated by its nature, however, a comprehensive figure of hysteresis can provide details of the inherent properties of the materials, magnetizing processes and their response to different magnetizing regimes. These are the key points in the design and analysis of the magnetic materials and electromagnetic devices.

1. *Magnetic energy loss and components*

Magnetic hysteresis loop is graphical presentation of hysteresis phenomenon whose area measure the specific energy loss per unit volume per cycle. Magnetic hysteresis loop is expressed by monitoring the instantaneous waveforms of the applied magnetic field strength $H(t)$ and flux density $B(t)$ for one cycle of the magnetization. Over the past decades, significant attempts have been made to develop dynamic models of the material. However considering the grain structure and anisotropic nature of the material, the proposed models do not represent physics of the material. Therefore, it is commonly acknowledged that dynamic performance of GO steels can be accurately analyzed based on the statistical energy loss separation developed by Bertotti [10]. In this approach, total energy loss of the material is separated into three components [17]:

$$W_{tot} = W_{hys} + W_{eddy} + W_{exc} \quad (1)$$

where, W_{hys} is hysteresis energy loss, W_{eddy} is classical eddy current energy loss and W_{exc} is excess energy loss. Energy loss analysis can be performed by analyzing the magnetic hysteresis for one magnetizing cycle, and hence, energy loss separation of (1) can be translated into magnetic field separation. In this approach, the instantaneous magnetic field strength at the lamination surface can be separated into hysteresis, eddy current and excess fields:

$$H(t) = H_{hys}(t) + H_{eddy}(t) + H_{exc}(t) \quad (2)$$

Using the dynamic models of the classical eddy current and excess fields, (2) leads the TSM for ferromagnetic material [20-21]:

$$H(t) = H_{hys}(B(t)) + \frac{d^2}{12\rho}\frac{dB}{dt} + g(B)\delta\left|\frac{dB}{dt}\right|^{\alpha} \quad (3)$$

where d is the lamination thickness and ρ is material resistivity. Directional parameter δ is $\delta = +1$ for $(dB/dt) > 0$, and $\delta = -1$ for $(dB/dt) < 0$. Exponent α designates the frequency dependence of the excess field component, and $g(B)$, in general, is a polynomial function of the flux density B to control shape of the modelled hysteresis loop.

The first term of (3), $H_{hys}(B(t))$ is the hysteresis field and can be calculated using any inverse static hysteresis model. To calculate this term, the conventional hysteresis dependence $B_{hys}(H)$ is represented in an inverse form $H_{hys}(B)$ [22]. It should be noted that, hysteresis field defined by the first term of (3) is independent from frequency (and time), but it depends on the instantaneous values of the magnetic field $B(t)$ for each magnetising frequency. The second term of (3) is the well-known classical eddy current field, calculated from the Maxwell equation for a homogenous medium with no grain or domain structure. Finally, the last term is excess field associated with the spatial distribution of domain walls and the microscopic eddy current loops concentrated around the moving domain walls [10, 23]. Excess loss component, as defined by Bertotti, is due to the magnetic microstructure of the material, e.g. grain size, crystallographic texture, and domain wall bowing. In GO steels, with relatively large grain size, excess energy loss counts for a significant amount of energy loss [18]. These three loss components are active simultaneously in any ferromagnetic material subjected to a time varying magnetic field. Fig 1 shows a simplified domain structure

of GO steel and construction of the eddy current loops associated with the classical eddy current and excess energy loss components.

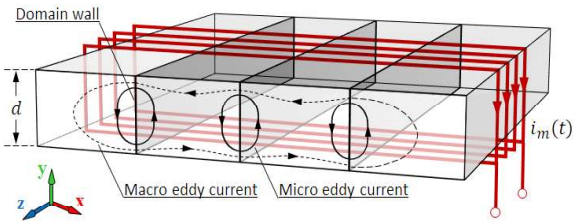

Fig 1 Perspective view of simplified domain structure of GO steel

2. *Magnetizing processes:*

Static or quasi-static hysteresis loop to represent the $H_{hys}(B)$ is the basis of the TSM, and hence, accurate modelling of the DHL requires an accurate figure of the SHL to model the first term in (3). This could be achieved experimentally or using a reliable analytical or numerical model. One practical technique to measure the SHL is to magnetize the material at a very low magnetizing rate to eliminate the dynamic fields $H_{eddy}(t)$ and $H_{exc}(t)$. Du and Robertson [23] assumed that the DHL measured at a low frequency of 5 Hz can adequately represent SHL of the material. Similar assumption has been made by other researchers to monitor SHL of magnetic materials under sinusoidal induction of low frequencies [6], [24-25]. This assumption, however, may result in uncertainties in the DHL modelling at low frequency ranges, e.g. power frequency 50/60 Hz, when it is implemented in the TSM. Zirka et. al. used a more accurate approach to measure quasi-static hysteresis loop of GO materials under controlled sinusoidal induction of 0.0033 Hz and 0.004 Hz [19-20]. Their results showed high accuracy in modelling the quasi-static hysteresis loop and energy loss analysis. It should be noted that measuring quasi-static hysteresis loop at low and very low frequencies may not be always feasible due to the requirement of special equipment or bandwidth limitation of the test setup.

An experimental procedure, with a different approach, was presented by Alonso, et. al. [26] to calculate quasi-static hysteresis loop of a single-phase toroidal transformer from the open circuit test. The calculated model was used in dynamic modelling of the magnetic core at three magnetizing frequencies: 60 Hz, 120 Hz and 180 Hz. This paper generalizes the proposed method in [26] to construct SHL of GO steels for dynamic modelling and energy loss analysis. The developed approach is in line with the phenomenology of magnetic hysteresis, and the phenomenological concepts of rate-dependent and rate-independent energy loss components of ferromagnetic materials under time varying magnetic fields.

Due to the dynamics of the magnetization processes under time varying magnetic field explained by the TSM (3), DHL of the material may follow different shapes, which essentially depend on the material properties and magnetization regime. The instantaneous values of the magnetic field strength $H(t)$ and flux density $B(t)$ cannot come up to the peak values simultaneously; which is more pronounced at low inductions and high frequencies [27-28]. Examples of DHLs for GO electrical steels, typically at a high flux density and a low flux density are shown in Figs 2-a and 2-b, respectively.

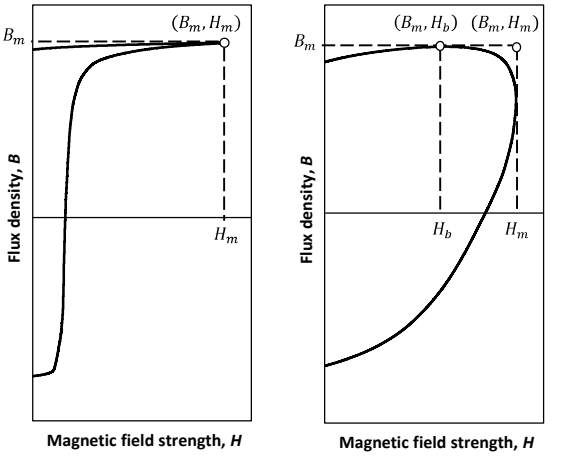

Fig 2 Dynamic hysteresis loops of GO electrical steel at a typical (a) high flux density and (b) low flux density

In Fig 2-a, where the material is magnetized near the saturation level, magnetic field strength $H(t)$ and flux density $B(t)$ come up to the peak values at the same instant. However, in the hysteresis loop of Fig 2-b, where the material is magnetized at a lower flux density, peak magnetic field strength H_m and peak flux density B_m occur at different instants. Therefore, in general, during one magnetizing cycle the material can experience two salient points with different concepts: $(B_m,\ H_m)$ where the instantaneous function of the flux density changes its direction, and $(B_m,\ H_b)$ where $dB/dt = 0$. Accordingly, by magnetizing the material over a continuous range of flux density from zero up to the saturation level, two distinctive curves can be observed [28]. An example of DHLs of a typical GO steel at a frequency of 50 Hz and peak flux densities of 0.1 T to 1.7 T, and the corresponding $(B_m,\ H_m)$ and $(B_m,\ H_b)$ curves are shown in Fig 3. Relative permeability of the material μ_r can be calculated by tracing the $(B_m,\ H_m)$ curve. This curve also provides magnetisation level of the material at a given frequency. $(B_m,\ H_b)$ curve, on the other hand, can provide more details about inherent properties of the material and magnetising processes which can be used in dynamic modelling and energy loss analysis.

According to the three components loss model (3), classical eddy current and excess magnetic fields are instantaneously proportional to dB/dt, while hysteresis

magnetic field is independent from dB/dt. At the instant where magnetic field strength comes up to H_b, the rate of magnetic flux density is practically vanished ($dB/dt = 0$), and dynamic energy loss components become zero, and hence, the total energy loss of the material is narrowed down to the hysteresis component only.

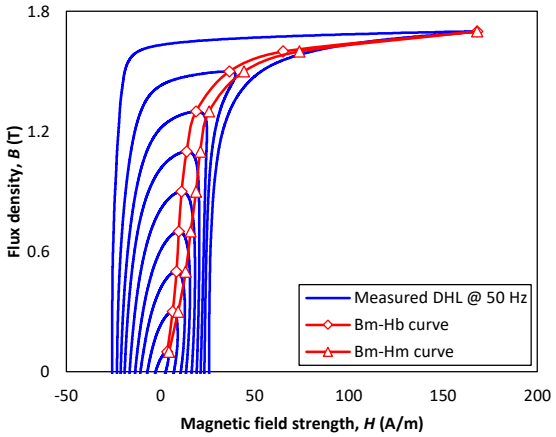

Fig 3 DHLs of GO steel at a frequency of 50 Hz and flux densities from 0.1 T to 1.7 T, and corresponding (B_m, H_m) and (B_m, H_b) curves

Phenomenology of the magnetic hysteresis and energy loss mechanism of ferromagnetic materials can be additionally speculated by the phenomenological concepts of rate-dependent and rate-independent energy loss components. According to (3) at (B_m, H_b) where $dB/dt = 0$, the instantaneous values of $H_{eddy}(t)$ and $H_{exc}(t)$ are zero and the magnetic field at the surface of the material is solely equal to the hysteresis field H_{hys}. As a phenomenological result, (B_m, H_b) curve can replicate the ascending branch of the SHL which is the basis of constructing the SHL. Dynamic model (3) also shows that how the material responds to the frequency of the magnetizing current. At very low and near zero magnetizing frequencies $dB/dt \approx 0$, and the applied magnetic field strength is solely to produce the hysteresis magnetic field H_{hys}, and total energy loss of the material would be the hysteresis loss only. By increasing frequency, the rate of dB/dt increases and the magnetic hysteresis responds to this by widening the loop area. Therefore, the instantaneous value of the ascending branch of the DHL at a particular frequency can be given by:

$$H_a(B(t)) = H_{hys}(B(t)) + H_{eddy}(B(t)) + H_{exc}(B(t)) \quad (4)$$

$$H_a(B(t)) = H_{hys}(B(t)) + H_{dyn}(B(t)) \quad (5)$$

and the hysteresis field can be calculated as:

$$H_{hys}(B(t)) = H_a(B(t)) - \Delta H_a \quad (6)$$

where ΔH_a is the horizontal difference between the SHL and DHL on the ascending branch at each particular flux density B, which is the magnetic field strength associated with the dynamic energy loss components. When the flux density $B(t)$ passes its peak, dB/dt turns to negative and the DHL turns to the descending branch. At a specific level of flux density for $dB/dt > 0$ and $dB/dt < 0$, the magnetising processes follow the same dynamic to shape the ascending and descending branches of the DHL, respectively. Therefore, equation (6) can be also used for the descending branch of the DHL:

$$H_{hys}(B(t)) = H_d(B(t)) - \Delta H_d \quad (7)$$

A graphical representation of equations (6) and (7) for a typical GO steel is shows Fig 4.

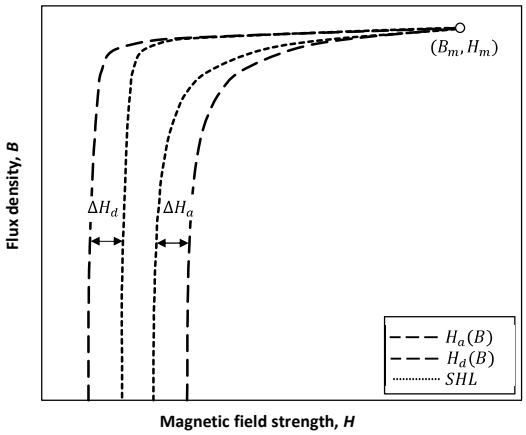

Fig 4 Frequency dependence of the ascending and descending branches of DHL for typical GO electrical steel

III.EXPERIMENTAL AND MODELLING RESULTS

Experimental work were performed on 0.3 mm thick GO 3 % SiFe with standard grades of M105-30P, and a measured resistivity of $\rho = 0.461$ μΩm. A standard double yoke SST was used to magnetize the test samples under controlled sinusoidal inductions from 5 Hz to 1 kHz, and peak flux densities of 0.1 T to 1.7 T. The test setup was calibrated to conform the reference standard BS EN 10280:2007 [4]. Uncertainty analysis of the measuring system was performed based on the recommendations given in UKAS M3003 [30]. Type A uncertainty was estimated at ± 0.30 %, and Type B uncertainty was estimated at ± 0.63 %. SHLs of the material were constructed using the developed approach in section II, and the DHLs were reproduced based on the TSM (3); the results are presented and discussed in the coming subsections.

1. Constructing the Static Hysteresis Loop (SHL):

Ascending branch $H_a(t)$ of the DHL for $B \geq 0$ at magnetising frequencies of 5 Hz, 10 Hz and 50 Hz and a peak flux density of $B_{pk} = 1.7\ T$ together with the measured $B_m - H_b$ curve are shown in Fig 5.

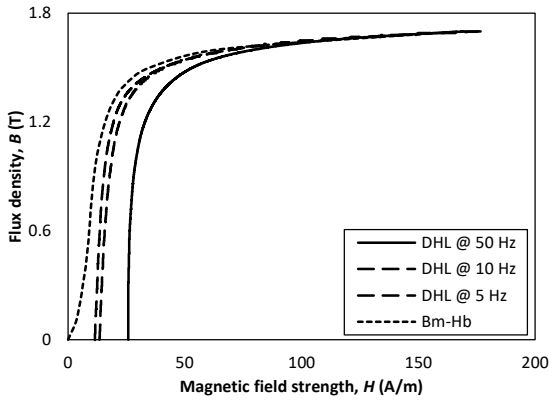

Fig 5 Ascending branch of the measured DHLs for $B \geq 0$ at a peak flux density of 1.7 T measured and $B_m - H_b$ curve

The horizontal distance ΔH_a between the ascending branches of the DHLs shows the magnetic field associated with the dynamic energy loss for the increased frequency. Fig 5 particularly shows that the rate of dB/dH of the DHLs follows the same trend, specifically at low frequencies e.g. 10 Hz and 5 Hz. In contrast, a comparison between the $B_m - H_b$ curve and the ascending branch of 5 Hz shows that, the $B_m - H_b$ curve is trending at slower rate for flux densities of $0 \leq B \leq 0.8\,T$, but it follows the same trend as for the DHL at higher inductions, i.e. $0.8\,T \leq B \leq 1.7\,T$. Therefore from this experiment, and for this particular material, the data points from the $B_m - H_b$ curve for $B \geq 0.8\,T$ can be used to construct the ascending branch of the SHL. This is the most important step in constructing the SHL. The lower part of the ascending branch of the SHL was constructed by extrapolating the data from the upper part. In this procedure the main objective is to maintain a sustain trend in the SHL by monitoring the rate of the dB/dH of the SHL and the measured DHL at 5 Hz. The constructed ascending branch of the SHL is shown in Fig 6. Finally, the descending branch of the SHL was calculated from (7), with the descending branch $H_d(B(t))$ at measured frequency of 5 Hz as the reference; the result is shown in Fig 7. Impact of the magnetizing frequency and rate-dependent magnetic field components on the loop area can be evidently seen from Fig 7.

Total energy loss calculated from the constructed SHL is 80.25 J/m^3, while the total energy loss calculated from the measured DHLs at frequencies of 5 Hz and 10 Hz are 104.14 and 114.47 J/m^3 per cycle, respectively. These results explicitly show that, low frequency hysteresis loops cannot be used as quasi-static hysteresis loop, and they may result in significant uncertainty in dynamic modelling of GO steels and energy loss separation. The constructed $B_{hys}(H)$ is reversible which mean it can be represented in an inverse form of $H_{hys}(B)$, as the basis of the dynamic modelling of GO steels using the TSM. For this purpose a simple algorithm was developed to reverse the $B_{hys}(H)$ dependency to $H_{hys}(B)$. To show accuracy of the constructed $H_{hys}(B)$, a comparison between the instantaneous wave shapes of the total magnetic field strength $H(t)$ and the hysteresis magnetic field $H_{hys}(B(t))$ at sinusoidal induction of 5 Hz and peak flux density of $B_{pk} = 1.7\,T$ is shown in Fig 8.

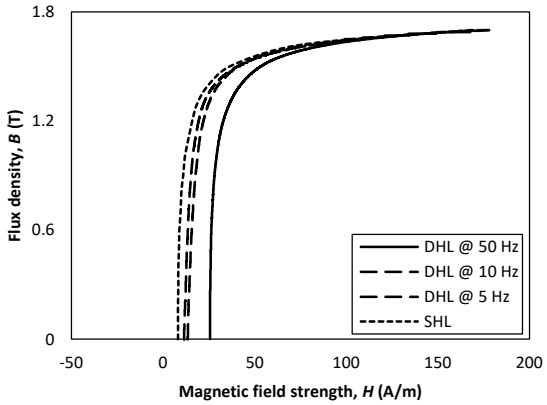

Fig 6 Ascending branch of the measured DHLs and constructed SHL for $B \geq 0$ at a peak flux density of 1.7 T

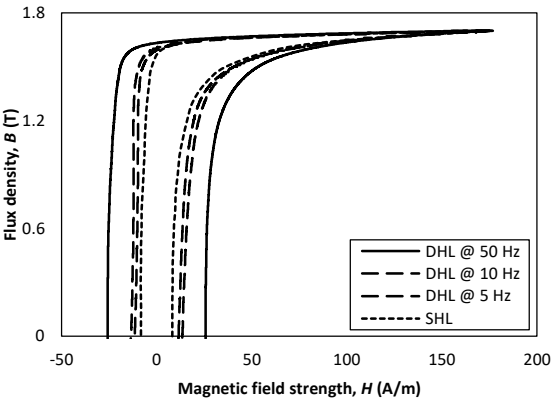

Fig 7 Constructed SHL and measured DHL at magnetizing frequencies of 5 Hz, 10 Hz and 50 Hz and a peak flux density of 1.7 T

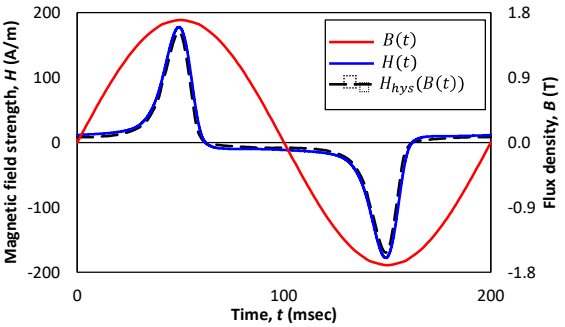

Fig 8 Instantaneous wave shapes of $H_{hys}(B(t))$, $H(t)$ and $B(t)$ at sinusoidal induction of 5 Hz and peak flux density of $B_{pk} = 1.7\,T$

It should be noted that, the magnetizing cycle of $H_{hys}(B(t))$ as shown in Fig 8 is not a physical cycle, but a mathematical description of the hysteresis phenomenon to link the hysteresis field to the dynamic components of the TSM (3) during one cycle of the magnetization. Fig 8 shows a close tendency between the total magnetic field strength $H(t)$ at magnetizing frequency of 5 Hz, and the constructed hysteresis magnetic field $H_{hys}(B(t))$. The difference between these two magnetic fields shows the effect of the magnetizing frequency on the rate-dependent magnetic field strength associated with the dynamic energy loss. More importantly, Fig 8 shows that both $H(t)$ and $H_{hys}(B(t))$ wave shapes follow the same trend during one magnetising cycle, i.e. $dH(t)/dt$ and $dH_{hys}(B(t))/dt$ are practically the same for each cycle of the magnetization. Therefore, the constructed SHL and the $H_{hys}(B(t))$ can be used in the dynamic modelling of GO steels to represent the magnetic field associated with the hysteresis energy loss. The developed technique was used to construct SHL and hysteresis magnetic field $H_{hys}(B(t))$ at lower flux densities, the results at peak flux densities of $B_{pk} = 1.1\ T$ to $B_{pk} = 1.7\ T$ are shown in Fig 9.

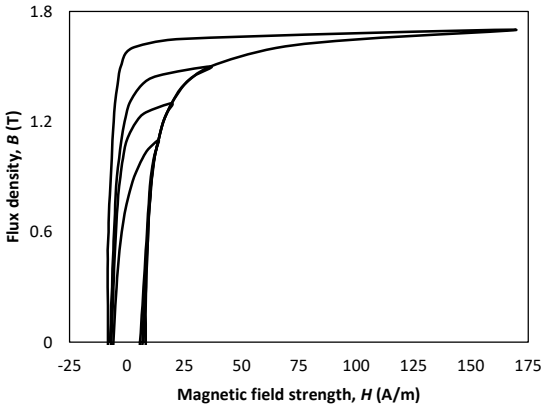

Fig 9 Constructed SHL at peak flux densities from 1.1 T to 1.7 T

According to the theory of TSM, a DHL of any frequency can be used to construct the SHL and hysteresis magnetic field $H_{hys}(B(t))$. However, due to uncertainty in some measuring systems at high frequencies, it is recommended to choose a low frequency DHL in this modelling. Furthermore, inherent properties and normal characteristics of electrical steels can be severely affected under high frequency magnetizations due to thermal effects, vibration, magnetostriction, etc. Therefore, to eliminate impacts of the rate-dependent components, this experiment should to be done at a low frequency. In this paper DHL of 5 Hz was implemented.

2. *Constructing the Dynamic Hysteresis Loop (DHL):*

DHLs of the samples were reproduced using model (3) where the constructed SHLs of Fig 9 were implemented to represent the hysteresis magnetic field. In a trial and error process, a constant exponent of $\alpha = 0.5$ was found acceptable for this material and this range of measurement. To fit the loop shape with the measured DHL, and more importantly to reproduce the magnetizing process and instantaneous function of the magnetic field strength $H(t)$, function $g(B)$ should be constructed for each portion of the measured DHLs [16-18]. Zirka et. al. [20] has empirically showed that a common feature of function $g(B)$ for GO steels is its minimum value at low $|B|$ and increasing values near the knee and close to the saturation level, and defined the following function for $g(B)$:

$$g(B) = G_m(1 + k_1 B^2) \tag{8}$$

where G_m and k_1 are two constant values to control shape of the modelled DHL at low $|B|$ and near the saturation, respectively. DHL modelling of the test sample was started at 50 Hz, where (8) was found as a proper function to replicated $g(B)$. The instantaneous waveforms of the total magnetic field strength $H(t)$, flux density $B(t)$ and three components of the TSM for one cycle of the frequency under controlled sinusoidal induction at peak flux densities of 1.1 T to 1.7 T, are shown in Fig 10. A comparison between the measured and calculated DHLs at peak flux densities of 1.1 T to 1.7 T is shown in Fig 11.

Fig 10 shows that at H_b, where $dB/dt = 0$, hysteresis field is at its maximum value, i.e. H_b coincides with the peak value of H_{hys} at all flux densities. Furthermore, Fig 11 shows that at high inductions, where H_m coincide with H_b, the ascending and descending branches of the DHL merge and coincide to the tip of the SHL at (B_m, H_m). At low inductions, where H_m differs from H_b, this phenomenon occurs at (B_m, H_b) point. This is a reliable means to validate the modelling results, specifically the constructed SHL, which is in line with the phenomenology of magnetic hysteresis outlined in section II.

Energy loss components of the material were calculated based on the modelled DHL of Fig 11; the results showed that hysteresis energy loss W_{hys}, classical eddy current energy loss W_{eddy}, and excess energy loss W_{exc} components account for 41 %, 24 % and 35 % of the total energy loss, respectively. These results are in compliance with the results reported by other researchers for 3 % SiFe GO steels at magnetizing frequency of 50 Hz and peak flux density of 1.7 T [19], [31-32].

To increase accuracy of the modelling at higher frequencies, a new empirical function with the general form of (9) was defined:

$$g(B) = G_m + k_1 B(B + k_2) \tag{9}$$

The designated computational functions of $g(B)$ at a peak flux density of $B_{pk} = 1.7\ T$ and magnetising frequencies of 100 Hz, 200 Hz, 400 Hz, 800 Hz and 1 kHz are given in (10) to (14) respectively. A comparison between the modelled and measured DHLs for the range of measurement is shown in Figs 12-a to 12-e, respectively.

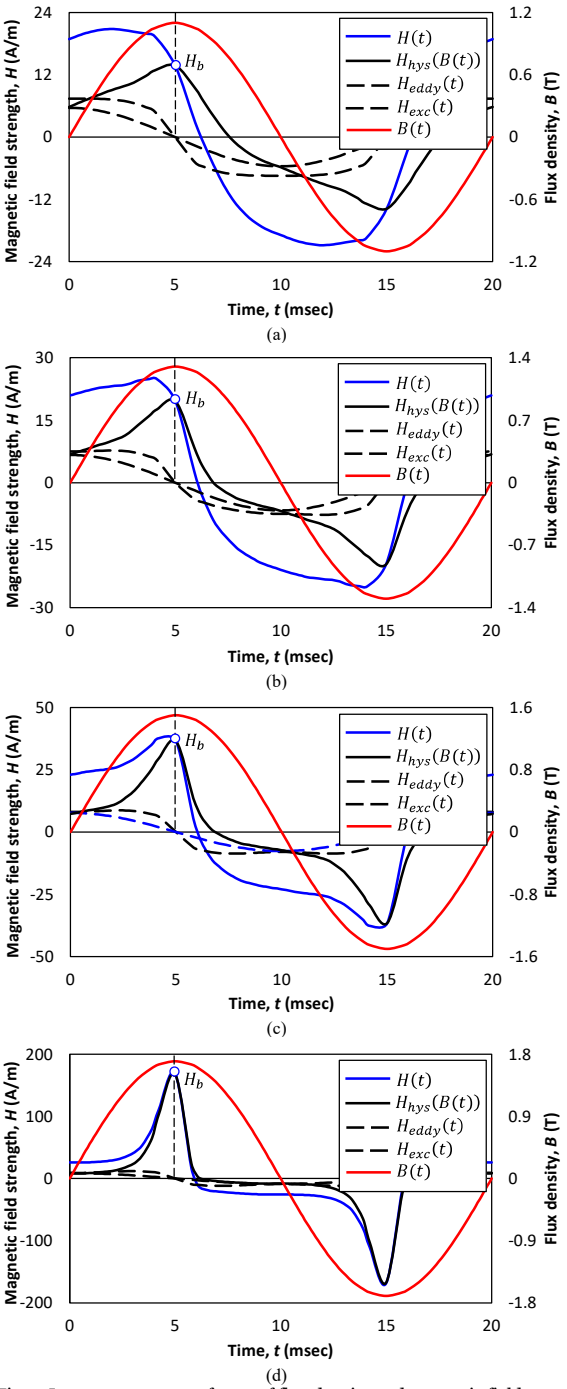

Fig 10 Instantaneous waveforms of flux density and magnetic field strength under sinusoidal induction of 50 Hz and at peak flux densities of (a) $B_{pk} = 1.1\ T$ (b) $B_{pk} = 1.3\ T$ (c) $B_{pk} = 1.5\ T$ and (d) $B_{pk} = 1.7\ T$

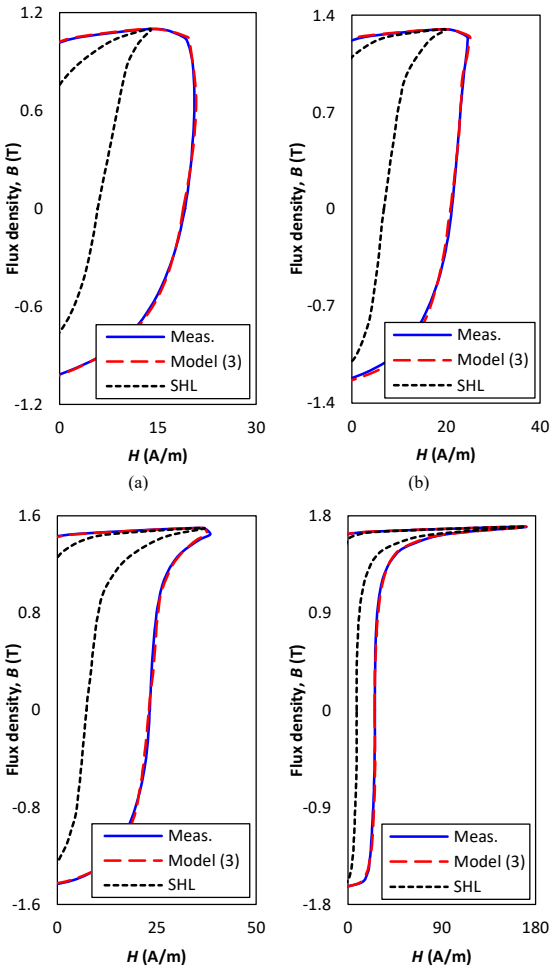

Fig 11 Comparison between the measured and modelled DHL at magnetizing frequency of 50 Hz and peak flux densities of (a) 1.1 T (b) 1.3 T (c) 1.5 T and (d) 1.7 T

$$g(B) = \begin{cases} 1.1 + 0.91B(B + 1.77) & -1.7 < B < -0.8 \\ 0.4 + 0.03B(B + 2.8) & -0.7 < B < 1.2 \\ 1 + B(B - 1.64) & 1.3 < B < 1.7 \end{cases} \quad (10)$$

$$g(B) = \begin{cases} 16.12 + 8.57B(B + 2.7) & -1.7 < B < -1.4 \\ 0.43 + 0.47B(B + 1.33) & -1.3 < B < -0.7 \\ 0.3 + 0.167B(B + 1.53) & -0.6 < B < 0.6 \\ 0.21 - 0.113B(B - 4.94) & 0.6 < B < 1.3 \\ -4.5 - 1.77B(B - 3.54) & 1.4 < B < 1.7 \end{cases} \quad (11)$$

$$g(B) = \begin{cases} 6.61 + 4.33B(B + 2.43) & -1.7 < B < -1.3 \\ 0.19 + 0.44B(B + 1.25) & -1.2 < B < 0.4 \\ 0.016 - 0.275B(B - 4.38) & 1.3 < B < 1.7 \end{cases} \quad (12)$$

$$g(B) = \begin{cases} -7.17 - 5B & -1.7 < B < -1.5 \\ 0.5 + 1.1B(B + 1.67) & -1.4 < B < -0.7 \\ 0.16 + 0.4B(B + 2.28) & -0.6 < B < 0.6 \\ -0.074 - 0.42B(B - 4.24) & 0.6 < B < 1.7 \end{cases} \quad (13)$$

$$g(B) = \begin{cases} 14.83 + 9B(B + 2.58) & -1.7 < B < -1.3 \\ 0.17 + 0.75B(B + 1.71) & -1.2 < B < -0.4 \\ 0.2 + 1.21B & -0.3 < B < 1.1 \\ 0.81 + 0.66B & 1.2 < B < 1.7 \end{cases} \quad (14)$$

Fig 12 explicitly shows accuracy of the calculated DHLs for the whole range of magnetization. Finally total energy loss per cycle was calculated from the measured and modelled DHLs. With the experimental results as the reference, the percentage difference between two sets of data were calculated; the results are shown and compared in Figs 13-a and 13-b, respectively. The highest error between the measured and calculated energy losses was found at magnetizing frequency of 50 Hz, where (8) was used to replicated $g(B)$. At higher frequencies where (9) was implemented, the error is practically negligible.

IV.CONCLUSION

Optimized design of magnetic cores for high efficiency electromagnetic devices, e.g. electric motors, transformers and reactors requires all aspects and concepts of power loss mechanism of the magnetic materials to be fully understood. Therefore, further understanding on the energy loss mechanism of the magnetic materials have been prioritized in the design and manufacturing of these devices. Dynamic behavior of ferromagnetic materials can be adequately analyzed by interpreting the hysteresis behavior and magnetizing processes of the materials. In this respect, experimental and analytical approaches have been widely proposed and successfully implemented by academic and industrial researchers. Most of these models starts by the static or quasi-static hysteresis models, to describe the hysteresis magnetic field and hysteresis energy loss. Magnetizing processes of ferromagnetic materials under time varying magnetic field is purely rate-dependent and, hence an in depth understanding about the dynamic behavior of the magnetic materials has important implications in characterization of the materials and their applications. This paper proposes a phenomenological approach to describe the magnetizing processes of GO electrical steels for practical range of magnetizations.

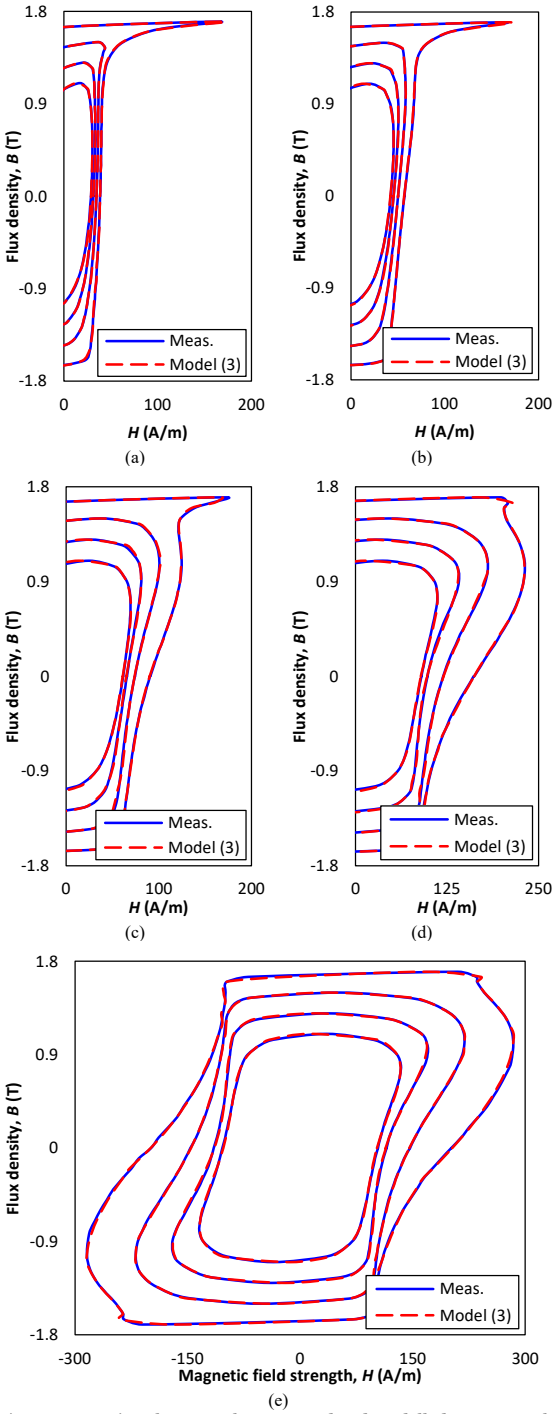

Fig 12 Comparison between the measured and modelled DHL at peak flux densities of 1.1 T to 1.7 T and magnetizing frequencies of (a) 100 Hz (b) 200 Hz (c) 400 Hz (d) 800 Hz and (e) 1 kHz

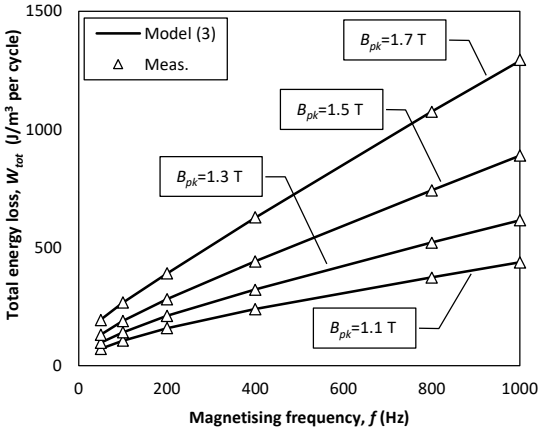

(a)

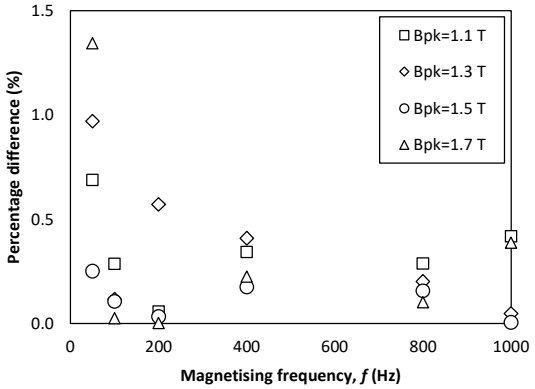

(b)

Fig 13 (a) Comparison between the calculated and measured energy losses (b) Percentage difference between the calculated and measured values

The proposed method is in line with the phenomenological concepts of rate-dependent and rate-independent energy loss of ferromagnetic materials under time varying magnetic field, to represent the static and dynamic magnetic fields. As the main objective of this work, static hysteresis loop of the material was constructed based on the measured hysteresis loops under contorted sinusoidal inductions. The proposed technique was validated to reproduce DHLs of GO electrical steel material at magnetizing frequencies from 50 Hz to 1 kHz and peak flux densities of 1.1 T to 1.7 T. This technique can be effectively used to analyze static and dynamic behaviors of GO steels and magnetic cores constructed from GO materials for this range of magnetization.

ACKNOWLEDGMENT

The author is grateful to Cogent Power Ltd. for providing the electrical steel materials and Cardiff University for the experimental data.

DATA AVAILABILITY

The data that support the findings of this study are available from the corresponding author upon reasonable request.

REFERENCES

[1] G. Bertotti, "Hysteresis in Magnetism, For Physicists, Materials Scientists and Engineers", Academic Press 1998
[2] G. Bertotti and I. Mayergoyz "The Science of Hysteresis", Academic Press 2005
[3] IEC 60404-2, Magnetic materials – Part 2: Methods of measurement of the magnetic properties of electrical steel strip and sheet by means of an Epstein frame, Edition 3.1, 2008-06
[4] BS EN 10280:2001 + A1:2007, Magnetic Materials - Methods of measurement of the magnetic properties of electrical sheet and strip by means of a single sheet tester
[5] F De Leon and A Semlyen, "A simple representation of dynamic hysteresis losses in power transformers," in IEEE Trans on Power Delivery, vol. 10, no. 1, pp. 315-321, Jan. 1995
[6] Daniels, T. Overboom and E. Lomonova, "Coupled statistical and dynamic loss prediction of high-permeability grain-oriented electrical steel", Eur. Phys. Journal Applied Physics, Vol. 90, Number 1, April 2020
[7] J. Takács, "A phenomenological mathematical model of hysteresis", COMPEL - The international journal for computation and mathematics in electrical and electronic engineering, Vol. 20 No. 4, pp. 1002-1015, 2001
[8] F. Preisach, "On the magnetic aftermath", Magazine for physics, volume 94 , pages 277 – 302, 1935
[9] Jiles and D Atherton "Theory of ferromagnetic hysteresis", JMMM, No. 61, 1986, pp. 48–60
[10] G. Bertotti, "General properties of power losses in soft ferromagnetic materials," in IEEE Trans. on Magn., Vol. 24, no. 1, pp. 621-630, Jan. 1988
[11] Liorzou, B. Phelps and D. L. Atherton, "Macroscopic models of magnetization," in IEEE Transactions on Magnetics, vol. 36, no. 2, pp. 418-428, March 2000
[12] R. Zeinali, D. C. J. Krop and E. A. Lomonova, "Comparison of Preisach and Congruency-Based Static Hysteresis Models Applied to Non-Oriented Steels," in IEEE Transactions on Magnetics, vol. 56, no. 1, pp. 1-4, Jan. 2020, Art no. 6700904
[13] Z. Li, J. Shan and U. Gabbert, "A Direct Inverse Model for Hysteresis Compensation," in IEEE Transactions on Industrial Electronics, vol. 68, no. 5, pp. 4173-4181, May 2021
[14] Vaseghi, D. Mathekga, S. Rahman, and A. Knight, "Parameter optimization and study of inverse J-A hysteresis model" IEEE Transactions on Magnetics, vol. 49, no. 5, pp. 1637–1640, May 2013
[15] S. Zirka, Y. Moroz, R. Harrison, and K. Chwastek, "On physical aspects of the Jiles-Atherton hysteresis models," J. Appl. Phys., vol. 112, no. 4, 2012, Art. no. 043916
[16] S. E. Zirka, Y. I. Moroz, P. Marketos and A. J. Moses, "Viscosity-based magnetodynamic model of soft magnetic materials," in IEEE Transactions on Magnetics, vol. 42, no. 9, pp. 2121-2132, Sept. 2006

[17] S. E. Zirka, Y. I. Moroz, P. Marketos, A. J. Moses and D. C. Jiles, "Measurement and Modeling of B-H Loops and Losses of High Silicon Nonoriented Steels," in IEEE Transactions on Magnetics, vol. 42, no. 10, pp. 3177-3179, Oct. 2006
[18] S. E. Zirka, Y. I. Moroz, P. Marketos, A. J. Moses, D. C. Jiles and T. Matsuo, "Generalization of the Classical Method for Calculating Dynamic Hysteresis Loops in Grain-Oriented Electrical Steels," in IEEE Transactions on Magnetics, vol. 44, no. 9, pp. 2113-2126, Sept. 2008
[19] S. Zirka, Y. Moroz, S. Steentjes, K. Hameyer, K. Chwastek, S. Zurek and R. Harrison "Dynamic magnetization models for soft ferromagnetic materials with coarse and fine domain structures", Journal of Magnetism and Magnetic Materials, Vol. 394, pp 229-236, Nov. 2015
[20] S. E. Zirka, Y. I. Moroz, A. J. Moses and C. M. Arturi, "Static and Dynamic Hysteresis Models for Studying Transformer Transients," in IEEE Transactions on Power Delivery, vol. 26, no. 4, pp. 2352-2362, Oct. 2011
[21] S. Steentjes, S. E. Zirka, Y. I. Moroz, E. Y. Moroz, and K. Hameyer, "A simplified model of ferromagnetic sheets considering the magnetization dynamics utilizing the saturation wave model", Journal of Applied Physics 115, 17D114 (2014)
[22] S. E. Zirka, Y. I. Moroz, N. Chiesa, R. G. Harrison and H. K. Høidalen, "Implementation of Inverse Hysteresis Model Into EMTP—Part II: Dynamic Model," in IEEE Transactions on Power Delivery, vol. 30, no. 5, pp. 2233-2241, Oct. 2015
[23] R. Du and P. Robertson, "Dynamic Jiles–Atherton Model for Determining the Magnetic Power Loss at High Frequency in Permanent Magnet Machines," in IEEE Transactions on Magnetics, vol. 51, no. 6, pp. 1-10, June 2015, Art no. 7301210
[24] Salvini and F. R. Fulginei, "Genetic algorithms and neural networks generalizing the Jiles–Atherton model of static hysteresis for dynamic loops", IEEE Trans. Magn., vol. 38, no. 2, pp. 873-876, Mar. 2002
[25] L. Santi, R. L. Sommer, A. Magni, G. Durin, F. Colaiori and S. Zapperi, "Dynamic hysteresis in Finemet thin films", IEEE Trans on Magn, Vol. 39, No. 5, pp. 2666-2668, Sep. 2003
[26] H Alonso, S Jazebi and F León, "Experimental Parameter Determination and Laboratory Verification of the Inverse Hysteresis Model for Single-Phase Toroidal Transformers," in IEEE Trans on Magn, Vol. 52, No. 11, pp. 1-9, Nov. 2016
[27] Z. Cheng, N. Takahashi, B. Forghani, Y. Du, Y. Fan, L. Liu, Z. Zhao, and H. Wang., "Effect of Variation of B-H Properties on Loss and Flux Inside Silicon Steel Lamination," in IEEE Trans on Magn, Vol. 47, No. 5, pp. 1346-1349, May 2011
[28] H. Hamzehbahmani, "A Phenomenological Approach for Condition Monitoring of Magnetic Cores Based on the Hysteresis Phenomenon," in IEEE Transactions on Instrumentation and Measurement, Vol. 70, pp. 1-9, 2021, Art no. 6003409
[29] H. Hamzehbahmani, "An Experimental Approach for Condition Monitoring of Magnetic Cores With Grain-Oriented Electrical Steels," in IEEE Transactions on Instrumentation and Measurement, Vol. 69, No. 6, pp. 3395-3402, June 2020
[30] UKAS M3003, "The Expression of Uncertainty and Confidence in Measurement", Edition 4, Oct 2019
[31] K. Foster, F. Werner, R. Del Vecchio, "Loss separation measurements for several electrical steels", Journal of Applied Physics Vol 53, Issue 11, pp 8308-8310, 1982
[32] S. E. Zirka, Y. I. Moroz, N. Chiesa, R. G. Harrison and H. K. Høidalen, "Implementation of Inverse Hysteresis Model Into EMTP—Part I: Static Model," in IEEE Transactions on Power Delivery, vol. 30, no. 5, pp. 2224-2232, Oct. 2015